

PRESSURE PULSES GENERATED BY CLOUD CAVITATION

G.E. Reisman and C.E. Brennen

California Institute of Technology
 Pasadena, Calif. 91125

ABSTRACT

This paper describes an experimental investigation of the large unsteady and impulsive pressures which are experienced on the suction surface of both an oscillating and static hydrofoil as a result of cloud cavitation. The present experiments used piezo-electric transducers to measure unsteady pressures at four locations along the chord of the foil and at two locations along the walls of the tunnel test section. These transducers measured very large positive pressure pulses with amplitudes of the order of tens of atmospheres and with durations of the order of tenths of milliseconds.

Two distinct types of pressure pulse were identified. "Local" pulses occurred at a single transducer location and were randomly distributed in position and time; several local impulses could be recorded by each transducer during an oscillation cycle. On the other hand, "global" impulses were registered by all the transducers almost simultaneously. Correlation of the transducer output with high speed movies of the cavitation revealed that they were produced by a large scale collapse of the bubble cloud. The location of the global impulses relative to the foil oscillation was quite repeatable and produced substantial far-field noise. The high speed movies also showed that the local impulses were caused both by crescent-shaped regions of low void fraction and by small bubbly structures. These regions appeared to be bounded by bubbly shock waves which were associated with the large pressure pulses.

The paper also quantifies the effect of reduced fre-

quency, cavitation number and tunnel velocity on the strength of the pressure pulses by presenting the acoustic impulse for a range of flow conditions. The reduced frequency is an important parameter in the determination of the total impulse level and the local and global pulse distribution. Large impulses are present on the foil surface even at cavitation numbers which do not result in large levels of acoustic radiation or global impulse. The total impulse increases with increasing tunnel velocity.

NOMENCLATURE

c	Chord length of foil (m)
C_p	Pressure coefficient, $(p - p_0)/\frac{1}{2}\rho U^2$
C_{pmin}	Minimum pressure coefficient
I	Acoustic impulse ($kPa.s$)
k	Reduced frequency, $\omega c/2U$
p	Fluid pressure (Pa)
p_0	Tunnel working section pressure (Pa)
p_a	Radiated acoustic pressure (Pa)
p_v	Vapor pressure
t	Time (s)
T	Period of foil oscillation (s)
U	Reference velocity of the flow (m/s)
α	Void fraction of the bubbly mixture
ρ	Density of the liquid
σ	Cavitation number, $(p_0 - p_v)/\frac{1}{2}\rho U^2$
ω	Foil oscillation frequency (rad/s)

INTRODUCTION

Cloud cavitation, often formed by the breakdown and collapse of a sheet or vortex cavity, is believed to be responsible for severe cavitation noise (see, for example, Reisman *et al.* 1994) and erosion damage (see Soyama *et al.* 1992). The generation of cavitation clouds may occur naturally as a result of the shedding of bubble-filled vortices, or it may be the response to a periodic disturbance imposed on the flow. Common examples of imposed fluctuations are the interaction between rotor and stator blades in a pump or turbine and the interaction between a ship's propeller and the non-uniform wake created by the hull.

Numerous investigators (Wade and Acosta 1966, Shen and Peterson 1978, 1980, Blake *et al.* 1977, Bark 1985, Franc and Michel 1988, Hart *et al.* 1990, Kubota *et al.* 1989, 1992, Le *et al.* 1993, de Lange *et al.* 1994) have studied the complicated flow patterns involved in the production and collapse of cloud cavitation on a hydrofoil. Recently, McKenney and Brennen (1994) qualitatively related the acoustic signature of a cavitating cloud to the dynamics of the unsteady cavitation on an oscillating hydrofoil. During an attendant study (Reisman *et al.* 1994), the magnitude of the sound level generated by cloud cavitation on an oscillating hydrofoil and its dependence on various parameters including cavitation number, σ , reduced frequency, k , and total air content, were measured.

Measurements of noise produced by cloud cavitation are characterized by pressure pulses of very short duration and large magnitude. These pressure pulses were observed in the work of Bark (1985), Bark and van Berlekom (1978), Le *et al.* (1993), McKenney and Brennen (1994), Reisman *et al.* (1994) and Shen and Peterson (1978, 1980). Very large magnitude pressure pulses were also measured by Avellan and Farhat (1989) during a study of cavitation vortex collapse. The large pressure pulses generated by cloud cavitation can be associated with shock waves propagating in the bubbly mixture. The structure of such bubbly shock waves was first explored by Noordij and van Wijngaarden (1974). Moreover, several years ago, Mørch, Kedrinskii and Hanson (Mørch 1980, 1981, Hanson *et al.* 1981) suggested that a cloud of cavitation bubbles collapses by the formation of a shock wave on the surface of the cloud and its subsequent inward propagation. It should also be noted that Jakobsen (1964) suggested that a static bubbly condensation shock occurs in the closure region of a large attached and bubbly cavity and provides the basic mechanism for cavity closure.

In the past, we have explored both the linear and weakly non-linear dynamics and acoustics of clouds of

cavitation bubbles (d'Agostino *et al.* 1988, 1989 and Kumar and Brennen 1991, 1992, 1993). More recently, we have employed the same set of governing equations to obtain numerical solutions for the fully non-linear growth and collapse of a cloud of cavitation bubbles (Wang and Brennen 1995). These calculations confirmed the formation of inward propagating shocks during collapse and demonstrated that very large pressure pulses are generated by the geometric focusing of these shocks. The radiated acoustic pressure was characterized by large magnitude pulses of short duration.

EXPERIMENTAL PROCEDURE

The experiments were conducted in the Low Turbulence Water Tunnel (LTWT) at Caltech, a closed-circuit facility with test section dimensions of $30.5\text{cm} \times 30.5\text{cm} \times 2.5\text{m}$ (Gates 1977). A modified NACA 0021 hydrofoil (with increased thickness between the mid-chord and the trailing edge) with a rectangular planform, a chord of 15.2cm and a span of 17.5cm , was reflection-plane mounted in the floor of the test section as described in Hart *et al.* (1990). A 750w DC motor is connected to the foil by a four-bar linkage such that it oscillates in pitch about an axis near the center of pressure, 0.38 of a chord from the leading edge. The mean angle of attack, the oscillation amplitude and frequency (up to 50Hz) are adjustable. An optical shaft encoder mounted to the DC motor provides a digital signal which was used to correlate the foil motion with the acoustic measurements and the high speed movies.

The unsteady pressures generated by the cavitation on the hydrofoil were measured by several transducers. A PCB model HS113A21 piezo-electric pressure transducer (bandwidth 100kHz) was mounted flush with the floor of the test section, 5cm downstream of the trailing edge of the foil (denoted later by #F). Another HS113A21 transducer was mounted in the tunnel ceiling at approximately the same axial location. Four PCB model 105B02 pressure transducers (bandwidth 50kHz , face diameter about 3mm) were recess-mounted inside the foil at locations 26% span from the foil root and 30%, 50%, 70% and 90% chord from the leading edge (denoted respectively by #1 through #4). By driving a transmitting hydrophone with a voltage impulse, the resonant frequencies of the transducer cavities were all determined to be about 35kHz . These values are in good agreement with the Helmholtz resonant frequency of 38kHz calculated for the recess. Great care was taken to avoid the presence of air bubbles in the cavities and the impulse response testing was able to confirm their absence by detecting any change in the

cavity resonant frequency. All data taken by the foil transducers was digitally low pass filtered at 20kHz to avoid any effect of cavity resonance. The transmitting hydrophone was also used along with a second receiving hydrophone to confirm the manufacturer's calibration of the foil transducers. The output signals from all six transducers were low pass filtered at 45kHz (to avoid aliasing) and recorded digitally at a sampling rate of 100kHz .

A good measure of the magnitude of the collapse pulses contained in the transducer output is the acoustic impulse, I (Ceccio and Brennen 1991, Kuhn de Chizelle *et al.* 1995), defined as the area under the pulse or

$$I = \int_{t_1}^{t_2} p_a(t) dt \quad (1)$$

where t_1 and t_2 are obtained from a threshold crossing method to identify the beginning and end of the pulse. A threshold of 20kPa was used for the floor and ceiling transducers while 200kPa was used for the foil surface transducers.

High speed movies with a framing rate of 500fps were taken to assist in the interpretation of the pressure transducer output. These movies were synchronized with the unsteady pressure measurements by triggering a timing light simultaneously with data acquisition commencement.

The data presented here were obtained from 40 samples at each operating condition where a single sample is defined by either one oscillation cycle or a 0.066sec time period in the case of the static foil experiments. The mean angle of attack was 5° , the oscillation amplitude was 5° . The foil was fixed at an angle of attack of 5° during the static foil experiments. Experiments were performed at cavitation numbers of 0.85, 0.95, and 1.05, at tunnel velocities of 7.5m/s , 8m/s and 8.5m/s and at reduced frequencies of 0, 0.76, 1.00 and 1.22. The total air content was 9.3ppm for the oscillating foil experiments and 8.2ppm for the static foil experiments.

CAVITATION STRUCTURE

A typical set of output signals from the transducers is shown in figure 1 which represents a single foil oscillation cycle with the origin corresponding to the maximum angle of attack. The output signals are characterized by very large amplitude pressure pulses of very short duration. As exemplified by figure 1, the magnitudes of these pulses are of the order of tens of atmospheres with typical durations of the order of tenths of milliseconds. As previously described by Reisman

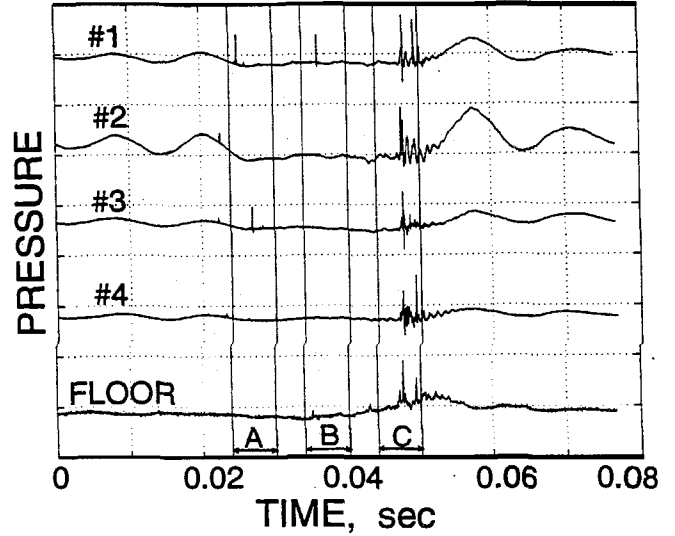


Figure 1: Typical transducer output during a single foil oscillation cycle. The top four traces are from the foil surface transducers and are numbered from the leading edge. The bottom signal is from the transducer mounted in the tunnel floor. The vertical axis scale is 1MPa/div. for the foil surface transducers and 100kPa/div. for the floor transducer. This typical data is for $\sigma = 0.95$, $k = 0.78$, $U = 8\text{m/s}$.

et al. (1994), the radiated acoustic pressure also contains pressure pulses which are illustrated by the bottom trace in figure 1. The magnitude of these pulses measured by the transducer in the tunnel floor is only on the order of one atmosphere. The closest approximation to the far field pressure is that measured by the transducer in the ceiling of the tunnel test section; this also contains impulses, but these pulses were of less than 10kPa in amplitude. Although these far field measurements are affected by both the directional dependence of the ceiling transducer and the tunnel test section acoustics, it is clear that there are order of magnitude differences in the amplitudes of the pulses measured on the foil, near the cavitating region and in the far field, respectively.

The low frequency variation present in the signal prior to the 0.025s mark and after the 0.05s mark was also observed at high cavitation numbers when the foil was fully wetted. This part of the signal is probably the result of stresses in the foil which are communicated through the transducer casings. This speculation is supported by the virtually instantaneous propagation of the low frequency disturbance and by the observation of similar signals even when the foil was oscillating in

air.

Two different types of pressure pulses were identified and can be illustrated by figure 1. The pulses occurring before the 0.04s mark are randomly distributed in time and space and are not repeated from cycle to cycle. We refer to these as *local* pulses. The pulses located between the 0.04s and 0.05s marks occur virtually simultaneously, are of higher amplitude and are repeated each cycle. We refer to these as *global* pulses; they produced substantial far-field noise and the location of the global impulses relative to the foil oscillation was quite repeatable.

The distinction between these two types of pressure pulse can be further elucidated by examining the high speed movies. These movies indicate that the local pulses are caused by local disturbances in the cavitation structure while global pulses are generated by a larger scale cloud cavitation collapse.

The various stages of the cavitation observed during a single oscillation cycle are depicted in figure 2. Inception occurs in the tip vortex and is soon followed by travelling bubble cavitation in the area of C_{pmin} . As the angle of attack increases, the bubbles coalesce into a single attached cavitation sheet which attains its maximum length as the angle of attack reaches a maximum. At this point, a re-entrant liquid jet penetrates the attached cavity from the downstream edge and propagates toward the leading edge of the foil. This re-entrant jet mechanism was first described by Knapp (1955) and further explored in the work of Lush and Skipp (1986), Kubota *et al.* (1992), and de Lange *et al.* (1994). The current observations, however, indicate that the process which occurs after the passage of the re-entrant jet is critical since the large pressure pulses are detected after the jet has reached the foil leading edge. The re-entrant jet breaks up the attached sheet cavity into a bubbly mixture which detaches from the foil surface and accelerates downstream. Local disturbances in the bubbly mixture are then observed and these structures have been correlated with the production of local pressure pulses, as explained in further detail below. Finally, the remains of the sheet cavity form a cloud of bubbles that undergo a coherent collapse as they are convected downstream. As shown later in this paper, this collapse results in only a slight change in the cloud radius but a large change in void fraction which propagates from the cloud perimeter to the cloud center.

Three specific intervals during the oscillation cycle are indicated in figure 1. Time interval *A* contains a local pulse in foil surface transducer #3. The cause of this pulse can be deduced from the high speed movie

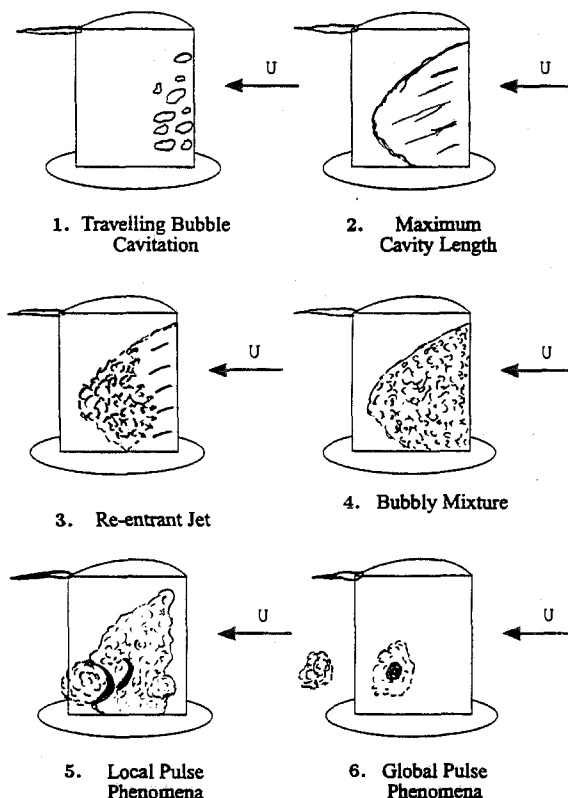


Figure 2: Cavitation structures observed during a single oscillation cycle. The angle of attack increases from sketch 1 to a maximum at sketch 2 and then decreases to a minimum at sketch 5.

frames in figure 3. The downstream edge of the crescent shaped region of low void fraction indicated by the arrow passes over transducer #3 between the two frames. The existence of this type of transient flow structure is a common occurrence during the detachment of a cavitation cloud from a sheet cavity as noted by Shen and Peterson (1978), Bark (1985), and McKenney and Brennen (1994). Examination of other high speed movies indicates the presence of a local pulse whenever the downstream edge of such a low void fraction structure passes over a transducer, and this observation is consistent with those of Shen and Peterson (1978). The transducer located near the trailing edge is an exception to this rule, but the cavitating region might be separated from the foil surface at this location. The boundaries of these low void fraction regions are observed to move both in the upstream and downstream directions relative to the bubbly flow as the region expands.

Time interval *B* and the corresponding movie frames of figure 4 contain a second kind of local pulse phenom-

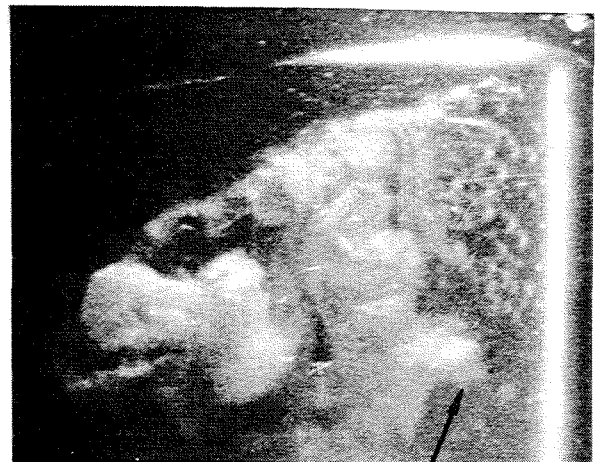
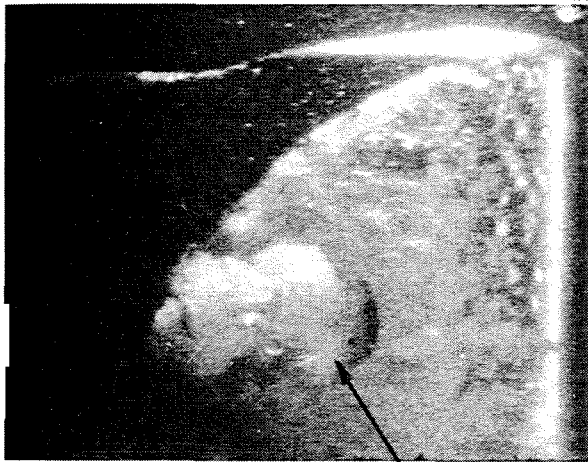
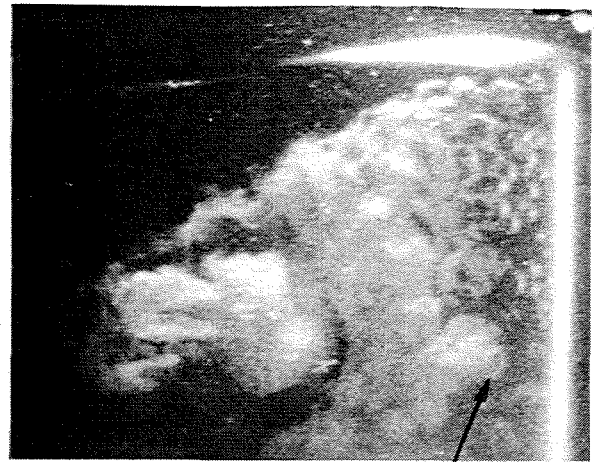


Figure 3: Crescent shaped flow structure of low void fraction. Consecutive high speed movie frames taken during time interval *A* of figure 1.

Figure 4: Local pulse generated by a small bubbly structure. Consecutive high speed movie frames taken during time interval *B* of figure 1.

ena. The local pulse in the output from transducer #1 corresponds to the passage of the upstream boundary of a local cavitation cloud indicated by the arrow in figure 4. Other movie and pressure data also show the presence of a local pulse when the upstream edge of a small bubbly structure passes the transducer. These local structures are created when the sheet cavity detaches from the foil. As with the first kind of local pulse, this second type is observed during a transition from a region of high void fraction to a region of low void fraction. The transitions which cause both types of local pulses are discrete and geometrically coherent.

Region *C* of figure 1 and the frames of figure 5 are representative of a global pulse. The cavitation cloud just upstream of the foil trailing edge undergoes a rapid and complete collapse between the two frames of figure

5. The collapse of this region radiates a pressure pulse which is detected by all of the foil transducers and the transducer located in the tunnel floor. It should be noted that this cloud collapse is similar to that calculated by Wang and Brennen (1995) in that it does not involve large changes in the overall dimensions of the cloud; rather collapse involves large changes in the void fraction within the cloud.

A typical set of output signals from the transducers during the static foil experiments is shown in figure 6. The magnitude of the observed pulses is much lower than those measured while the foil was oscillating; they were typically only a few atmospheres in amplitude. There was a substantial reduction in the radiated noise, and only local events were observed. No global pulses were produced when the foil was stationary. The shedding of bubble clouds from the downstream edge of the

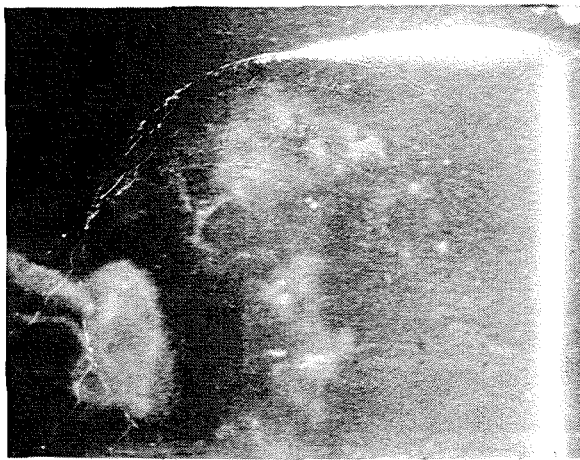
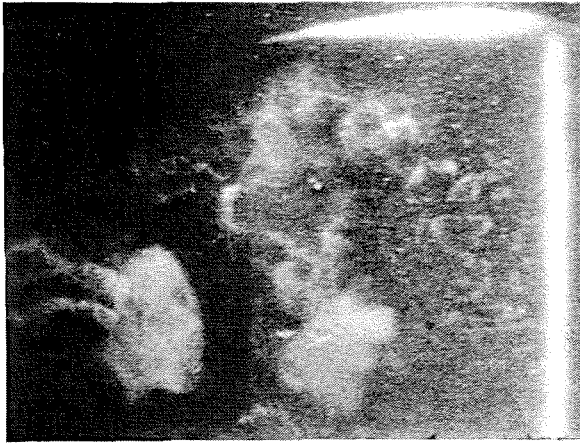


Figure 5: Global cloud collapse. Consecutive high speed movie frames taken during time interval *C* of figure 1.

attached cavity was not characterized by any particular frequency; rather the clouds were detached in a continuous process.

IMPULSE MEASUREMENTS

The experimental results depicted in figures 7 through 11 illustrate the variation of the average acoustic impulses with reduced frequency, cavitation number and tunnel velocity for both the static and the oscillating foil. In each figure the calculated impulses are presented for both the global and local pressure pulses detected by the four foil mounted transducers and the transducer located in the tunnel test section floor. Each average acoustic impulse presented in the figures is based on data collected during 40 individual foil oscillation cycles.

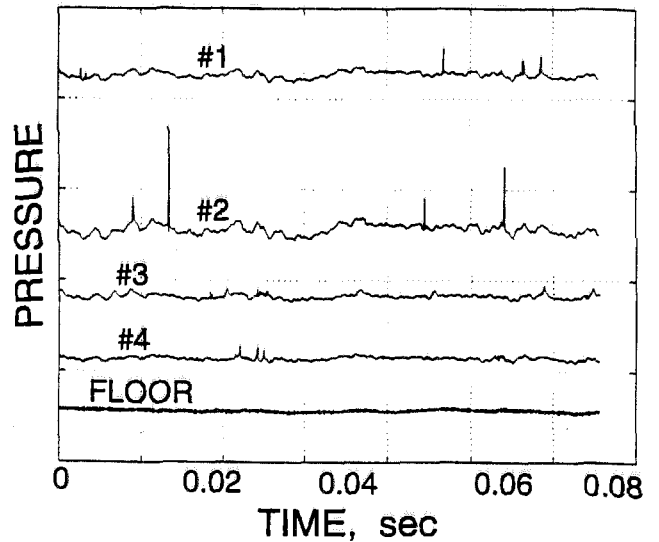


Figure 6: Typical transducer output during static foil experiments. The top four traces are from the transducers mounted on the foil and are numbered from the leading edge. The bottom signal is from the transducer mounted in the tunnel floor. The vertical axis scale is 500 kPa/div. for the foil surface transducers and 50 kPa/div. for the floor transducer. This typical data is for an angle of attack of 5° , $\sigma = 0.85$, $U = 8 \text{ m/s}$.

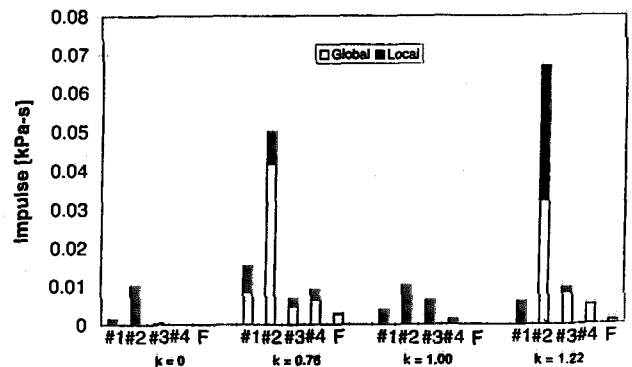


Figure 7: Effect of the reduced frequency, k , on the impulse, I . Data for $\sigma = 0.95$ and $U = 8 \text{ m/s}$.

Figure 7 illustrates the variation in the magnitudes of the local and global impulses with reduced frequency at a constant cavitation number, σ , and tunnel velocity, U . Note that, with the exception of #2 at $k = 1.22$, the magnitudes of the local impulses are quite independent of the reduced frequency and are therefore similar for

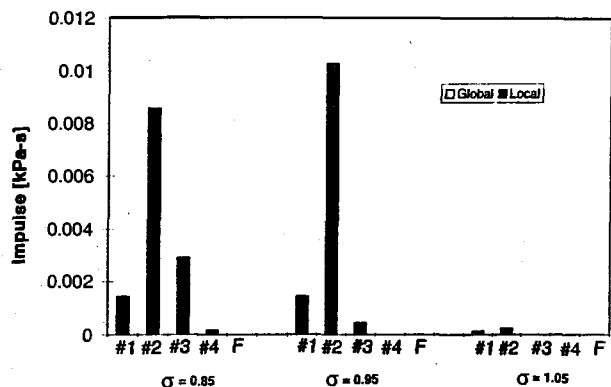


Figure 8: Effect of cavitation number, σ , on the impulse, I . Data for the static foil at an angle of attack of 5° and $U = 8m/s$.

the static and oscillating foils. On the other hand global impulses are virtually non-existent with the static foil under the conditions of figure 7. On the oscillating foil, there appears to be a broad range of reduced frequencies around unity in which the coherent collapses associated with global pulses are triggered. As seen in figure 7, there also appear to be specific frequencies like $k = 0.76$ and $k = 1.22$ which seem to produce the maximum global impulses. This general pattern of variation with reduced frequency is similar to that seen in the radiated noise by McKenney and Brennen (1994) and Reisman *et al.* (1994); note that the radiated noise measured by the floor transducer is only substantial when global pulses are present. We also note from figure 7 that the spatial distribution of the measured impulses is similar for all reduced frequencies; they tend to be larger at mid-chord where the sheet cavitation breaks up and collapses.

Figures 8 and 9 illustrate the variations in the impulses with the cavitation number, σ , for the static and oscillating foils, respectively. With the static foil, the local impulses appear rather suddenly when σ is reduced below about 1.00. The largest impulses occur near transducer #2, close to the cavity closure region; however, as σ is decreased to 0.85 the values at #3 increase as the cavitation collapse extends to that location. Le *et al.* (1993) also noted that the largest pulses on their static foil occurred near cavity closure.

When the foil is oscillating, the global impulses produced are also very sensitive to changes in cavitation number with the largest global impulses occurring in the middle of the cavitation number range. A similar effect was detected in the radiated impulses by McKenney and Brennen (1994) and Reisman *et al.* (1994), but

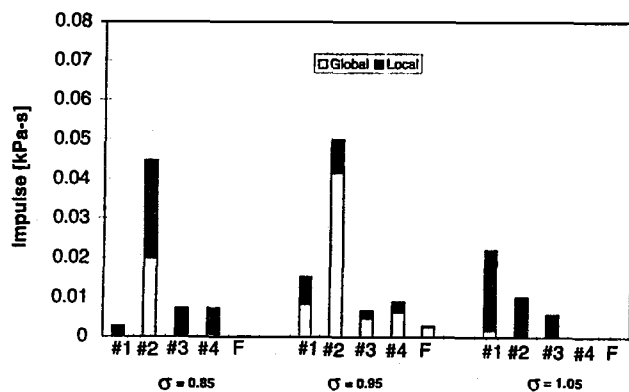


Figure 9: Effect of the cavitation number, σ , on the impulse, I . Data for the oscillating foil with $k = 0.76$ and $U = 8m/s$.

the occurrence of cloud cavitation in the present experiments is more sensitive to changes in σ , perhaps due to the larger thickness of the present foil.

It is important to note that extremely large *local* pressure pulses occur at cavitation numbers which do not produce global shocks. An average local acoustic impulse in excess of $0.025kPa.s$ is observed on #2 in figure 9 at $\sigma = 0.85$. This flow condition is characterized by sheet cavitation which extends well beyond the trailing edge of the foil and does not produce large radiated pressure pulses outside of the cavitating region.

Both with the static foil and with the oscillating foil (at high cavitation numbers), large local impulses occur on the foil surface without any substantial radiated impulse being registered by the floor transducer. This suggests that significant cloud cavitation damage could occur on a foil which is not exhibiting large acoustic radiation. Conversely, global pulses always produce substantial radiated noise which is registered by the floor transducer.

The effects of the magnitude of the tunnel velocity are illustrated in figures 10 and 11 for the static and oscillating foils, respectively (in the latter case, since the foil oscillation frequency was held constant at $12.7Hz$, there is also a small variation in the reduced frequency as the tunnel velocity changes). With the static foil, the local impulses increase rapidly with increasing velocity as one would expect since cavitation noise normally scales with the velocity raised to some large power. Note again the predominance of events near transducer #2. The imposition of oscillation changes this pattern. Note in figure 11, that the total impulse increases as the tunnel velocity is increased at constant σ . This occurs at every measuring location with the single exception of the value measured by the #2 transducer at

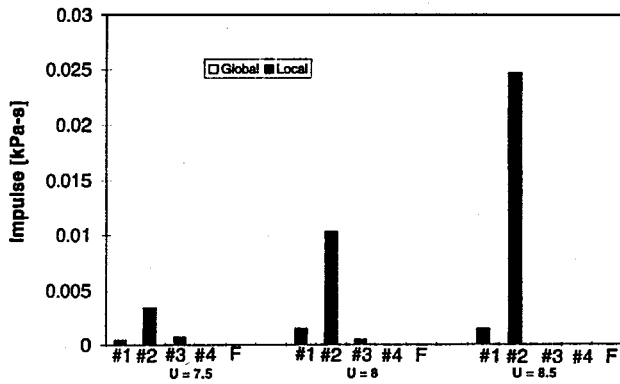


Figure 10: Effect of tunnel velocity, U , on the impulse, I . Data for a fixed angle of attack of 5° and $\sigma = 0.95$.

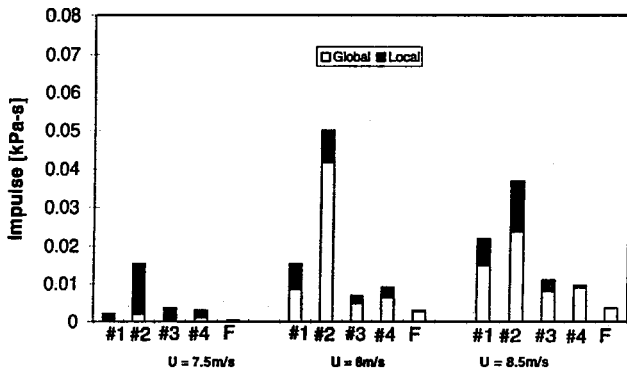


Figure 11: Effect of the tunnel velocity, U , on the impulse, I . Data for $\sigma = 0.95$ and $0.72 < k < 0.81$.

$U = 8.5\text{m/s}$. The almost universal increase is primarily due to a growth in the global acoustic impulse. Unlike the behavior with the static foil, the local impulse magnitudes remain fairly constant as the tunnel velocity is changed.

CONCLUSIONS

This paper has examined the large positive pressure impulses which occur on the surface of a hydrofoil during cloud cavitation; both static and oscillating foils were investigated. The pulses were shown to have magnitudes on the order of tens of atmospheres with typical durations of the order of tenths of milliseconds. Pressure pulses of similar magnitude were observed by Le *et al.* (1993), who measured pulse magnitudes of up to 7MPa on a stationary foil at $\sigma = 0.81$, $U = 12\text{m/s}$ and an angle of attack of 4.8° . Their experiments used flush-mounted transducers with face diameters of 1mm

and bandwidths over 300kHz .

However, these pulse magnitudes are significantly greater than those measured by Shen and Peterson (1978) who detected pulses with magnitudes comparable to the dynamic pressure, (up to 110kPa). There are at least two explanations for this discrepancy. Both the amplitude of foil oscillation (up to 1.55°) and the mean angle of attack (3.25°) were significantly less than those of the current experiments. Also, the transducers used by Shen and Peterson (1978) had a bandwidth of only 2kHz . The short duration impulses measured in our experiments have a broadband frequency content with substantial contributions above 2kHz .

The radiated pulse magnitudes measured by Bark (1985) and Bark and van Berlekom (1978) were on the order of tens of kPa , but these were measured off the foil surface. These are similar to our far field measurements but are significantly smaller than the impulse amplitudes measured by the transducer mounted in our water tunnel floor. This reduction in amplitude may be attributed to the significantly lower velocities of the Bark and van Berlekom experiments which were performed at 5m/s . It should be noted that our surface pressure measurements are several orders of magnitude lower than the massive impulses observed by Avellan and Farhat (1993) which averaged 900MPa in amplitude with extreme values as high as 2200MPa .

High speed movies indicated the presence of a re-entrant jet which, as previously described by Knapp (1955) and a number of recent investigators, penetrates the sheet cavity as the cavity reaches its maximum length. The jet then breaks the cavity into a bubbly mixture which detaches from the foil surface. In the present study, pressure pulses of either type were only detected after the passage of the re-entrant jet.

Furthermore, an examination of the movies led to the identification of two distinct types of pressure pulses. "Local" pulses, which are registered by a single transducer, are randomly distributed in time and space and are not repeated from cycle to cycle. Local pulses are caused at a given transducer location by the passage of either crescent-shaped regions of low void fraction or small bubbly structures. In either case, they are observed during a transition from a region of high void fraction to a region of low void fraction. The crescent-shaped regions are similar to the "depressions in the cavity surface" noted by Shen and Peterson (1978) and the "deep inward buckling of the cavity interface" observed by Bark (1985). The discrete boundaries of the crescent-shaped regions and the motion of these boundaries relative to the bubbly flow suggest that these boundaries are bubbly shock waves. The collapse of va-

por bubbles within these waves could explain the large pressure impulses measured on the foil surface.

On the other hand, "global" pulses, which occur almost simultaneously on all four transducers, are of higher amplitude, radiate substantial far field noise and are repeated at the same point of each oscillation cycle. Global pulses are caused by large scale cloud cavitation collapse and were not observed on the static foil.

By calculating the acoustic impulse, a quantitative measure of the effect of reduced frequency, k , cavitation number, σ , and tunnel velocity on the strength of the pressure pulses was obtained. The reduced frequency is an important parameter in the determination of the total impulse level and the local and global pulse distribution. The cavitation number has a significant effect on the global impulse strength, but large impulses are still present on the foil surface at values of σ where acoustic radiation is minimal and global pulses are rare or non-existent. The changes with tunnel velocity were significantly different for the stationary and oscillating foils. The local impulses on the stationary foil increased greatly with tunnel velocity and the global impulses on the oscillating foil did likewise. However, the local impulses on the oscillating foil did not change so dramatically with tunnel velocity. We also note that the spatial distribution of the impulse measurements, while highly influenced by the cavitation number, are virtually independent of the reduced frequency and tunnel velocity.

It seems clear that both the local and global surface pressure pulses could contribute to foil damage. Indeed, the very large magnitudes of these surface impacts could be responsible for the foil damage reported by Morgan (1995), who observed trailing edges bent away from the suction surface and toward the pressure surface.

The calculations of spherical cloud collapse by Wang and Brennen (1994) confirm that shock wave formation is an integral part of the collapse of such a cloud. Of course, most clouds are far from spherical. Nevertheless, the collapse of all or parts of non-spherical clouds will produce points at which shock waves focus to produce large radiated pulses. However, it is not currently clear what three-dimensional forms the propagating shocks might take in the highly non-uniform bubbly environments which occur in real flows. The experimental observations do suggest that the bubbly region near the surface may act as a wave-guide for the propagation of the crescent-shaped shock structures associated with local impulses. Much clearly remains to be understood regarding these structures and their consequences.

ACKNOWLEDGMENTS

We wish to thank John Van Deusen and Rodney Rojas for their help in fabricating the foil. The authors are also very grateful for the assistance provided by Amir Alagheband, Amy Herr, Don Kwak, Tricia Waniewski and Cecilia Lin. We are also deeply appreciative of the support of the Office of Naval Research who sponsored this research under grant number N00014-91-J-1295.

REFERENCES

- Avellan, F. and Farhat, M., 1989, "Shock pressure generated by cavitation vortex collapse," ASME Int. Symp. on Cavitation Noise and Erosion in Fluid Systems, FED-Vol.88, pp. 199-125.
- Bark, G. and Berlekom, W.B., 1978, "Experimental investigations of cavitation noise," Proc. 12th ONR Symp. on Naval Hydrodynamics, pp. 470-493.
- Bark, G., 1985, "Developments of distortions in sheet cavitation on hydrofoils," Proc. ASME Int. Symp. on Jets and Cavities, pp. 470-493.
- Blake, W.K., Wolpert, M.J. and Geib, F.E., 1977, "Cavitation noise and inception as influenced by boundary-layer development on a hydrofoil," *J. Fluid Mech.*, Vol. 80, pp. 617-640.
- Ceccio, S.L. and Brennen, C.E., 1991, "Observations of the dynamics and acoustics of travelling bubble cavitation," *J. Fluid Mech.*, Vol. 233, pp. 633-660.
- d'Agostino, L. and Brennen, C.E., 1988, "Acoustical absorption and scattering cross-sections of spherical bubble clouds," *J. Acoust. Soc. Am.*, Vol. 84, pp. 2126-2134.
- d'Agostino, L. and Brennen, C.E., 1989, "Linearized dynamics of spherical bubble clouds," *J. Fluid Mech.*, Vol. 199, pp. 155-176.
- de Lange, D.F., de Bruin, G.J. and van Wijngaarden, L., 1994, "On the mechanism of cloud cavitation - experiment and modelling," Proc. 2nd Int. Symp. on Cavitation, Tokyo, Japan, pp. 45-50.
- Franc, J.P. and Michel, J.M., 1988, "Unsteady attached cavitation on an oscillating hydrofoil," *J. Fluid Mech.*, Vol. 193, pp. 171-189.
- Gates, E. M., 1977, "The influence of freestream turbulence, freestream nuclei populations, and a drag-reducing polymer on cavitation inception on two axisymmetric bodies," PhD thesis, Cal. Inst. of Tech.
- Hanson, I., Kedrinskii, V.K. and Mørch, K.A., 1981, "On the dynamics of cavity clusters," *J. Appl. Phys.*, Vol. 15, pp. 1725-1734.
- Hart, D.P., Brennen, C.E. and Acosta, A.J., 1990, "Observations of cavitation on a three dimensional os-

illating hydrofoil," *ASME Cavitation and Multiphase Flow Forum*, FED-Vol. 98, pp. 49-52.

Jakobsen, J.K., 1964, "On the mechanism of head breakdown in cavitating inducers," *ASME J. Basic Eng.*, Vol. 86, pp. 291-304.

Knapp, R.T., 1955, "Recent investigations of the mechanics of cavitation and cavitation damage," *Trans. ASME*, Vol. 77, pp. 1045-1054.

Kubota, A., Kato, H., Yamaguchi, H. and Maeda, M., 1989, "Unsteady structure measurement of cloud cavitation on a foil section using conditional sampling," *ASME J. Fluids Eng.*, Vol. 111, pp. 204-210.

Kubota, A., Kato, H., Yamaguchi, H. and Maeda, M., 1992, "A new modeling of cavitating flows - a numerical study of unsteady cavitation on a hydrofoil section," *J. Fluid Mech.*, Vol. 240, pp. 59-96.

Kuhn de Chizelle, Y., Ceccio, S.L. and Brennen, C.E., 1995, "Observations, scaling and modelling of travelling bubble cavitation", *J. Fluid Mech.*, Vol. 293, pp. 99-126.

Kumar, S. and Brennen, C.E., 1991, "Non-linear effects in the dynamics of clouds of bubbles," *J. Acoust. Soc. Am.*, Vol. 89, pp. 707-714.

Kumar, S. and Brennen, C.E., 1992, "Harmonic cascading in bubble clouds," *Proc. Int. Symp. on Propulsors and Cavitation*, Hamburg, pp. 171-179.

Kumar, S. and Brennen, C.E., 1993, "Some nonlinear interactive effects in bubbly cavitating clouds," *J. Fluid Mech.*, Vol. 253, pp. 565-591.

Le, Q., Franc, J.P. and Michel, J.M., 1993, "Partial cavities: pressure pulse distribution around cavity closure," *ASME J. Fluids Eng.*, Vol. 115, pp. 249-254.

Lush, P.A. and Skipp, S.R., 1986, "High speed cine observations of cavitating flow in a duct," *Int. J. Heat Fluid Flow*, Vol. 7, No. 4, pp. 283-290.

McKenney, E.A. and Brennen, C.E., 1994, "On the dynamics and acoustics of cloud cavitation on an oscillating hydrofoil," *Proc. ASME Symp. on Cavitation and Gas-Liquid Flows in Fluid Machinery and Devices*, FED-Vol.190, pp. 195-202.

Morgan, W.B., 1995, personal communication.

Mørch, K.A., 1980, "On the collapse of cavity cluster in flow cavitation," *Proc. First Int. Conf. on Cavitation and Inhomogeneties in Underwater Acoustics*, Springer Series in Electrophysics, Vol. 4, pp. 95-100.

Mørch, K.A., 1981, "Cavity cluster dynamics and cavitation erosion," *Proc. ASME Cavitation and Polyphase Flow Forum*, pp. 1-10.

Noordij, L. and van Wijngaarden, L., 1974, "Relaxation effects, caused by relative motion, on shock waves in gas-bubble/liquid mixtures," *J. Fluid Mech.*, Vol. 66, pp. 115-143.

Reisman, G.E., McKenney, E.A. and Brennen, C.E., 1994, "Cloud cavitation on an oscillating hydrofoil," *Proc. 20th ONR Symp. on Naval Hydrodynamics*, pp. 78-89.

Shen, Y.T. and Peterson, F.B., 1978, "Unsteady cavitation on an oscillating hydrofoil," *Proc. 12th ONR Symp. on Naval Hydrodynamics*, pp. 362-384.

Shen, Y.T. and Peterson, F.B., 1980, "The influence of hydrofoil oscillation on boundary layer transition and cavitation noise," *Proc. 13th ONR Symp. on Naval Hydrodynamics*, pp. 221-241.

Soyama, H., Kato, H. and Oba, R., 1992, "Cavitation observations of severely erosive vortex cavitation arising in a centrifugal pump," *Proc. Third I.Mech.E. Int. Conf. on Cavitation*, pp. 103-110.

Wade, R.B. and Acosta, A.J., 1966, "Experimental observations on the flow past a plano-convex hydrofoil," *ASME J. Basic Eng.*, Vol. 88, pp. 273-283.

Wang, Y.-C. and Brennen, C.E., 1995, "The noise generated by the collapse of a cloud of cavitation bubbles," *ASME Symp. on Cavitation and Gas-Liquid Flows in Fluid Machinery and Devices*, FED-Vol.226, pp. 17-29.